

Supplementary Information

Synthesis and photophysical properties of photostable 1,8-naphthalimide dyes incorporating benzotriazole-based UV absorbers

Toshiyuki Uesaka,^{*ab} Tomoyuki Ishitani,^a Takahito Shimeno,^c Naoya Suzuki,^b Shigeyuki Yagi^b and Takeshi Maeda,^{*b}

a Shipro Kasei Kaisha, LTD., Mikuni-cho, Sakai-shi, Fukui 913-0036, Japan. E-mail: t-uesaka@shiprokasei.com

b Department of Applied Chemistry, Graduate School of Engineering, Osaka Prefecture University, Naka-ku, Sakai 599-8531, Japan. E-mail: tmaeda@chem.osakafu-u.ac.jp

c Shin-Nakamura Chemical Co., LTD., Wakayama-shi 640-8390, Japan.

Contents

1. Characterization data
2. Absorption and fluorescence spectra in various solvents
3. Phosphorescence spectra
4. DFT calculations
5. Properties of PMMA Films
6. NMR and MS spectra

1. Characterization data

1.1 Compound 1

Melting point: over 300 °C. ^1H NMR (600 MHz, DMSO- d_6): δ 10.51 (s, 1H), 10.46 (s, 1H), 8.77-8.78 (d, J = 8.4 Hz, 1H), 8.56-8.57 (d, J = 7.2 Hz, 1H), 8.51-8.52 (d, J = 7.2 Hz, 1H), 8.35-8.36 (d, J = 8.4 Hz, 1H), 8.04-8.05 (m, 2H), 7.93-7.95 (m, 2H), 7.53-7.56 (m, 3H), 7.18-7.21 (dd, J = 8.4, 8.4 Hz, 1H), 2.30 (s, 3H). ^{13}C NMR (125 MHz, DMSO- d_6): δ 170.19, 164.11, 163.52, 148.38, 144.19 (2C), 141.05, 132.81, 132.19, 131.42 (2C), 130.02, 129.56, 129.04, 128.03 (2C), 126.97, 126.27, 125.84, 124.73, 123.50, 119.94, 119.74, 118.60 (2C), 24.67. FT-IR (ATR, cm^{-1}): 3240, 3040, 1708, 1670, 1538, 1371, 1340, 1239, 1197, 780, 748, 734. MS (ESI) m/z : $[\text{M}+\text{Na}]^+$ Calcd for $\text{C}_{26}\text{H}_{17}\text{N}_5\text{NaO}_4$ 486.12; Found 486.08. Anal. Calcd for $\text{C}_{26}\text{H}_{17}\text{N}_5\text{O}_4$: C, 67.38; H, 3.70; N, 15.11. Found: C, 67.43; H, 4.02; N, 15.17.

1.2 Compound 3

Melting point: over 300 °C. ^1H NMR (600 MHz, DMSO- d_6): δ 10.46 (s, 1H), 10.31 (s, 1H), 8.78-8.79 (d, J = 8.4 Hz, 1H), 8.57-8.58 (d, J = 7.8 Hz, 1H), 8.52-8.53 (d, J = 8.4 Hz, 1H), 8.36-8.37 (d, J = 8.4 Hz, 1H), 8.14-8.16 (m, 2H), 7.93-7.95 (dd, J = 7.8, 7.8 Hz, 1H), 7.73-7.74 (d, J = 1.8 Hz, 1H), 7.52-7.54 (dd, J = 1.8, 8.4 Hz, 1H), 7.48-7.50 (dd, J = 2.1, 8.7 Hz, 1H), 7.10-7.12 (d, J = 9.0 Hz, 1H), 2.30 (s, 3H), 1.31 (s, 9H). ^{13}C NMR (125 MHz, DMSO- d_6): δ 170.17, 164.47, 163.89, 149.40, 144.27, 143.70, 142.59, 141.06, 135.46, 132.26, 131.49, 130.01, 129.60, 129.45, 128.78, 127.49, 126.95, 124.72, 123.44, 122.79, 119.92, 119.16, 118.75, 118.52, 118.02, 34.49, 31.69 (3C), 24.66. FT-IR (ATR, cm^{-1}): 3249, 2959, 1668, 1657, 1377, 1240, 1195, 779. MS (ESI) m/z : $[\text{M}+\text{H}]^+$ Calcd for $\text{C}_{30}\text{H}_{26}\text{N}_5\text{O}_4$ 520.20; Found 520.19. Anal. Calcd for $\text{C}_{30}\text{H}_{25}\text{N}_5\text{O}_4$: C, 69.35; H, 4.85; N, 13.48. Found: C, 69.13; H, 5.16; N, 13.24.

1.3 Compound 4

Melting point: over 300 °C. ¹H NMR (600 MHz, DMSO-*d*₆): δ 10.43 (s, 1H), 8.74-8.75 (d, *J* = 7.8 Hz, 1H), 8.51-8.53 (d, *J* = 7.2 Hz, 1H), 8.46-8.48 (d, *J* = 7.8 Hz, 1H), 8.33-8.34 (d, *J* = 7.8 Hz, 1H), 7.90-7.92 (dd, *J* = 8.1, 8.1 Hz, 1H), 7.52-7.53 (d, *J* = 7.8 Hz, 2H), 7.27-7.28 (d, *J* = 7.8 Hz, 2H), 2.29 (s, 3H), 1.35 (s, 9H). ¹³C NMR (150 MHz, DMSO-*d*₆): δ 170.16, 164.36, 163.79, 150.95, 140.93, 133.87, 132.19, 131.40 (2C), 129.88, 129.27, 129.06 (2C), 126.90, 126.19, 124.63, 123.31, 119.87, 118.42, 34.98, 31.73 (3C), 24.64. FT-IR (ATR, cm⁻¹): 3332, 2951, 1712, 1663, 1506, 1374, 1237, 1199, 783, 562. MS (ESI) *m/z*: [M+Na]⁺ Calcd for C₂₄H₂₂N₂NaO₃ 409.15; Found 409.11. Anal. Calcd for C₂₄H₂₂N₂O₃: C, 74.59; H, 5.74; N, 7.25. Found: C, 74.73; H, 5.88; N, 7.32.

1.4 Compound 5

Melting point: 129 °C. ¹H NMR (600 MHz, DMSO-*d*₆): δ 10.53 (s, 1H), 8.02-8.04 (m, 2H), 7.80-7.81 (dd, *J* = 1.8, 8.4 Hz, 1H), 7.52-7.54 (m, 2H), 7.42-7.45 (m, 1H), 7.16-7.17 (d, *J* = 7.8 Hz, 1H), 7.03-7.06 (dd, *J* = 8.1, 8.1 Hz, 1H). ¹³C NMR (150 MHz, DMSO-*d*₆): δ 151.47, 144.09 (2C), 131.65, 131.63, 127.87 (2C), 125.83, 120.09, 118.52 (2C), 118.44. FT-IR (ATR, cm⁻¹): 3097, 1490, 1256, 1221, 741, 684, 656, 472. MS (ESI) *m/z*: [2M-H]⁻ Calcd for C₂₄H₁₇N₆O₂ 421.14; Found 420.57. Anal. Calcd for C₁₂H₉N₃O: C, 68.24; H, 4.29; N, 19.89. Found: C, 68.59; H, 4.46; N, 19.94.

1.5 Compound 6

Melting point: 153°C. ¹H NMR (500 MHz, DMSO-*d*₆): δ 10.51 (s, 1H), 8.07-8.08 (m, 2H), 7.54-7.57 (m, 3H), 7.15 (s, 1H), 3.47 (br, 2H), 1.71 (s, 2H), 1.34 (s, 6H), 0.74 (s, 9H). ¹³C NMR (125 MHz, DMSO-*d*₆): δ 143.76 (2C), 142.11, 138.96, 129.87, 128.29 (2C), 126.69, 119.18, 118.49

(2C), 115.07, 56.60, 38.40, 32.64, 32.14 (3C), 31.76 (2C). FT-IR (ATR, cm^{-1}): 3445, 3364, 3059, 2955, 1512, 1219, 751, 725, 659. MS (ESI) m/z : $[\text{M}]^+$ Calcd for $\text{C}_{20}\text{H}_{26}\text{N}_4\text{O}$ 338.21; Found 338.56.

2. Absorption and fluorescence spectra in various solvents

Table S1 Optical properties of **1-5** and the equimolar mixture of **4** and **5** in various solvents.^a

Compd	Solvent	λ_{abs} (nm)	ϵ_{max}	λ_F (nm)	λ_{EX} (nm)	Stokes shift (cm^{-1})	Φ_F (%)	τ (ns) (χ^2) ^d	k_r (ns^{-1})	k_{nr} (ns^{-1})
1	CH ₃ OH	337	27000	466	370	5570	56.2	5.2 (1.03)	0.11	0.084
	CHCl ₃	340	27700	443	372	4310	27.8	2.1 (1.09)	0.13	0.34
	DMSO	370	16200	464	373	5260	27.8	2.5 (1.07)	0.11	0.28
2	CH ₃ OH	342	28000	468	373	5440	7.5	0.79 (1.01)	0.10	1.2
	CHCl ₃	350	28500	473	379	5240	2.8	1.4 (1.02)	0.020	0.68
	DMSO	364	17600	465	375	5160	7.4	0.68 (1.04)	0.11	1.4
3	CH ₃ OH	356	20200	466	376	5140	41.7	4.3 (1.06)	0.10	0.14
	CHCl ₃	359	31500	444	380	3790	5.1	0.82 (1.08)	0.062	1.2
	DMSO	371	17700	464	375	5120	39.1	2.8 (1.02)	0.14	0.22
4^b	CH ₃ OH	364	14900	465	368	5670	82.6	7.3 (1.04)	0.11	0.024
	CHCl ₃	365	15100	444	370	4510	46.5	2.9 (1.02)	0.16	0.19
	DMSO	374	15000	464	373	5260	54.6	3.8 (1.09)	0.14	0.12
5^c	CH ₃ OH	328	17300	392	313	6440	0.8	0.057 (1.08)	0.14	18
	CHCl ₃	333	18600	392	315	6240	0.6	1.1 (1.04)	0.0054	0.90
	DMSO	289	13100	419	285	11220	1.2	0.26 (1.05)	0.046	3.8
4 + 5^b	CH ₃ OH	335	13400	468	370	5660	87.1	8.1 (1.05)	0.11	0.016
	CHCl ₃	339	15300	444	372	4360	48.2	3.2 (1.09)	0.15	0.16
	DMSO	372	8000	464	374	5190	56.5	4.2 (1.05)	0.14	0.10

^aConc. 20 μM . ^bConc. 30 μM . ^cConc. 50 μM . ^dLifetimes were determined by fitting the decay curves with a single-exponential decay function. The quantities that express the mismatch between data and fitted function (χ^2) are shown in parentheses.

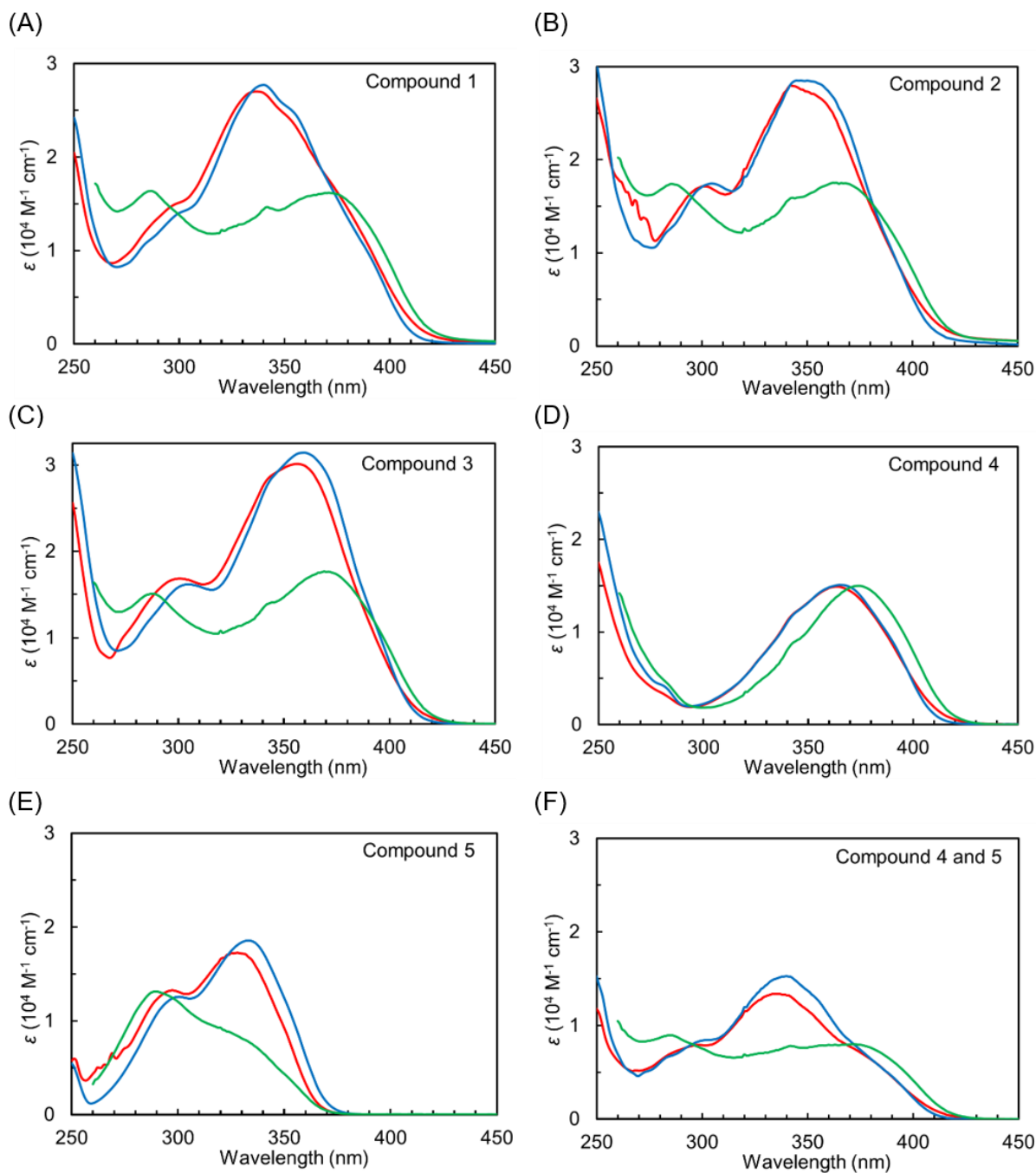


Fig. S1 UV-vis absorption spectra of **1** (A), **2** (B), **3** (C), **4** (D), **5** (E), and the equimolar mixture of **4** and **5** (F) in CH_3OH (red), CHCl_3 (blue), and DMSO (green).

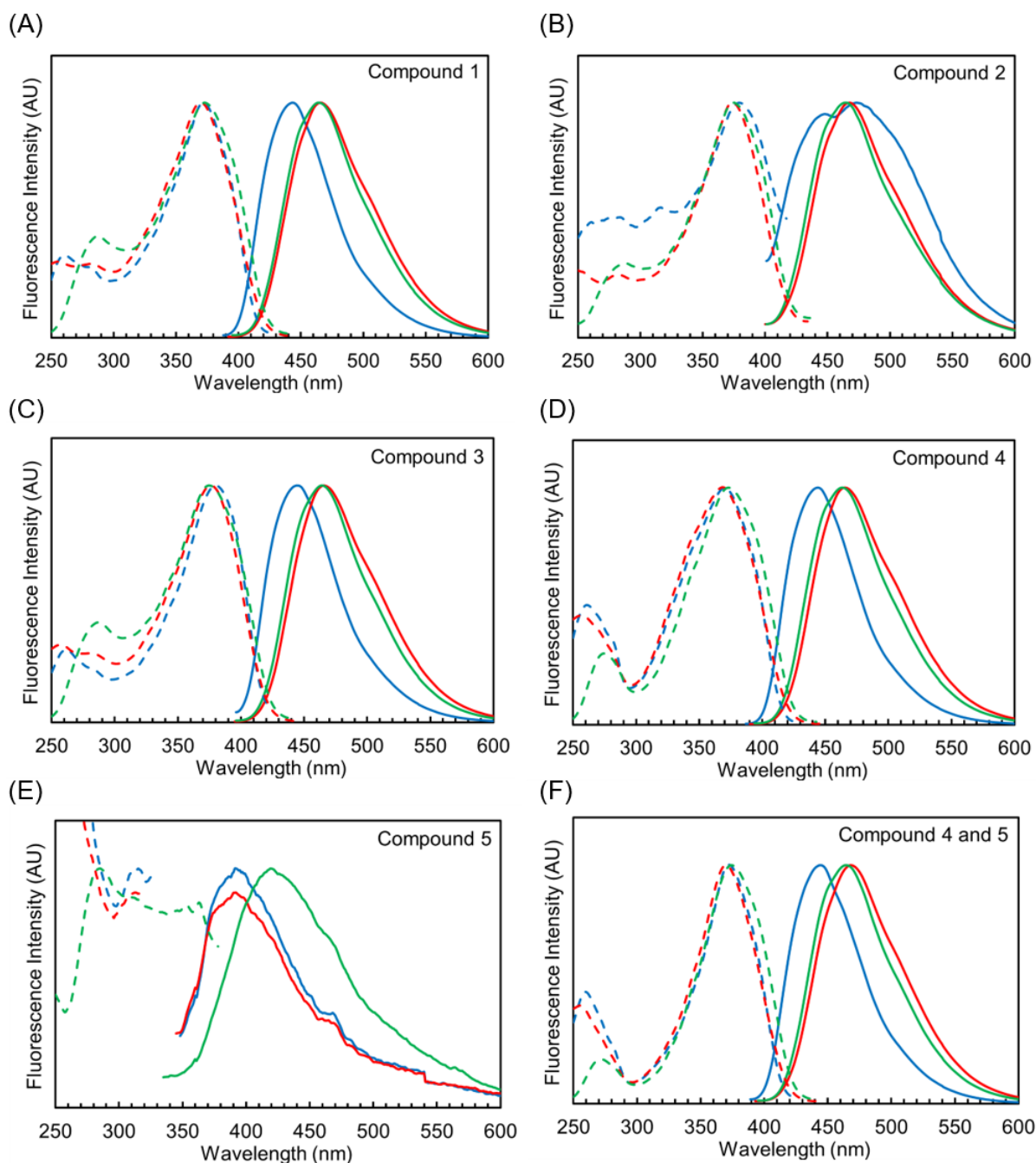


Fig. S2 Fluorescence (solid-line) and excitation (dot-line) spectra of **1** (A), **2** (B), **3** (C), **4** (D), **5** (E), and the equimolar mixture of **4** and **5** (F) in CH₃OH (red), CHCl₃ (blue), and DMSO (green).

3. Phosphorescence spectra

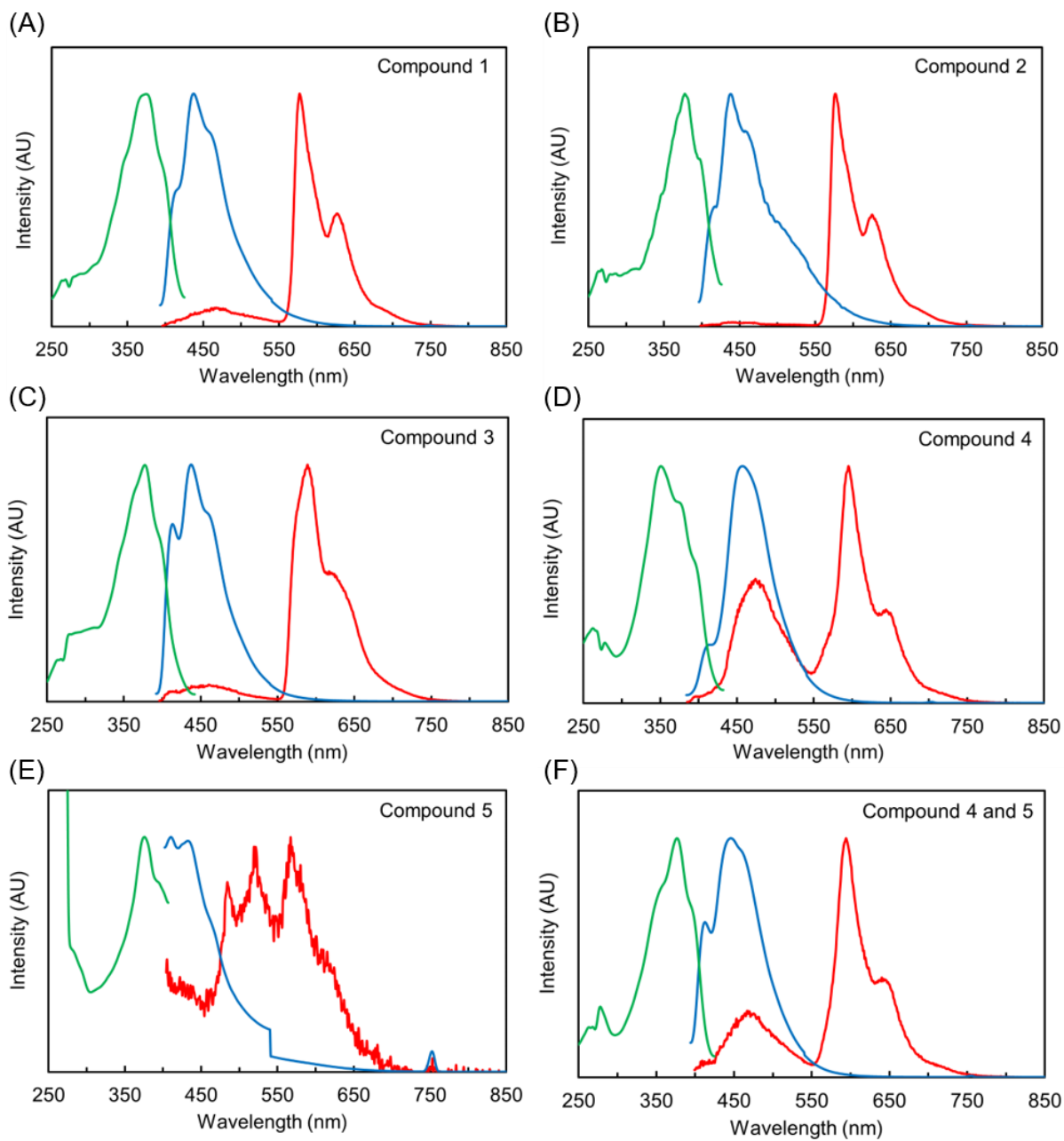


Fig. S3 Phosphorescence (red), fluorescence (blue), and excitation (green) spectra of **1** (A), **2** (B), **3** (C), **4** (D), **5** (E), and the equimolar mixture of **4** and **5** (F) in toluene at 77 K.

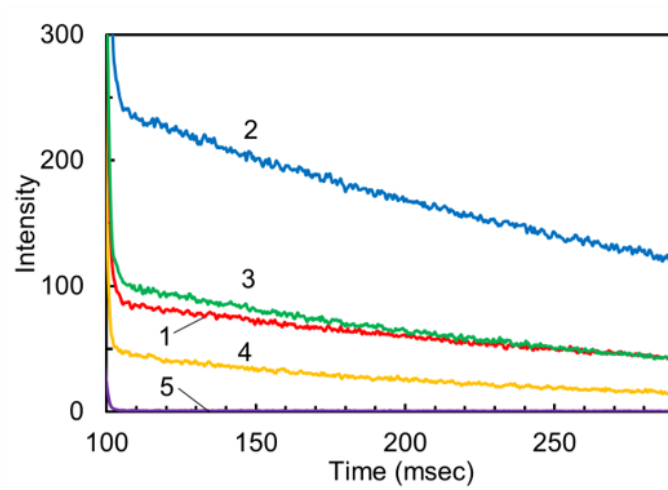


Fig. S4 Phosphorescence lifetimes of 1-5. After 100 msec, the excitation light was shut off.

4. DFT calculations

The geometries of the ground states and excited states for **1-3** were optimized in CH₃OH by DFT and time-dependent DFT (TD-DFT) calculations with the Gaussian 09 program.¹ The calculations were performed with the CAM-B3LYP exchange-correlation functional under a 6-31G+(d) basis set.

Table S2 Geometrical parameters and total energies of optimized structures for S₀, neutral S₁, and zwitterionic S₁ of **1-3** calculated at the CAM-B3LYP/6-31G+(d) (solvent: CH₃OH). The calculations of **2** were performed on the models in which 1,1,3,3-tetramethylbutyl groups were replaced with *tert*-butyl groups.

Compd	Optimized structures	$\varphi_{\text{BTA-NI}}$ (°) ^a	$\varphi_{\text{BT-PH}}$ (°) ^b	C-N (Å) ^c	O-H (Å) ^d	N-H (Å) ^e	Total energies (hartree)
1	S ₀	87.4	0.23	1.44	0.99	1.76	-1575.01637
	neutral S ₁	87.9	0.35	1.43	0.99	1.76	-1574.89759
	zwitterionic S ₁	85.0	11.2	1.43	1.99	1.02	-1574.89575
2	S ₀	87.6	0.14	1.44	0.99	1.76	-1732.17643
	neutral S ₁	87.0	0.16	1.44	0.99	1.76	-1732.05764
	zwitterionic S ₁	86.7	13.7	1.43	2.02	1.02	-1732.05857
3	S ₀	87.3	1.82	1.44	0.99	1.78	-1732.17562
	neutral S ₁	87.0	1.09	1.44	0.99	1.78	-1732.05707
	zwitterionic S ₁	88.6	15.6	1.44	2.01	1.03	-1732.05817

^aDihedral angles between the 2-(2-hydroxyphenyl)-2*H*-benzotriazole and the 1,8-naphthalimide.

^bDihedral angles between the benzotriazole group and the phenyl group.

^cBond lengths between the carbon atom of the 2-(2-hydroxyphenyl)-2*H*-benzotriazole and the nitrogen atom of the 1,8-naphthalimide.

^dBond lengths of the hydroxy group.

^eBond lengths between the nitrogen atom of the benzotriazole group and the hydrogen atom of the hydroxy group.

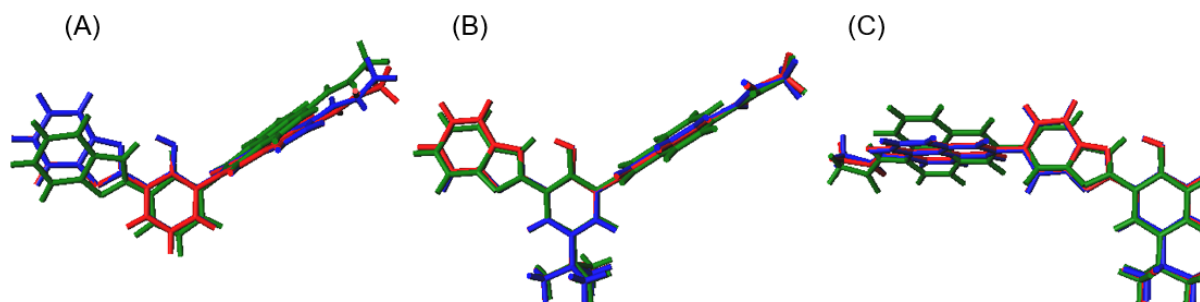


Fig. S5 Comparisons of the optimized structures of the S₀ (red), the neutral S₁ (blue), and the zwitterionic S₁ (green) for **1** (A), **2** (B), and **3** (C) calculated at the CAM-B3LYP/6-31G+(d) (solvent: CH₃OH). The calculations of **2** were performed on the models in which 1,1,3,3-tetramethylbutyl groups were replaced with *tert*-butyl groups.

5. Properties of PMMA Films

Table S3 Optical properties of **1-5** and the equimolar mixture of **4** and **5** in PMMA films^a.

Compd	λ_{abs} (nm)	λ_F (nm)	λ_{EX} (nm)	Stokes shift (cm ⁻¹)	Φ_F (%)
1	340	449	375	4400	32.7
2	349	475	403	3760	17.9
3	361	450	389	3490	19.6
4	370	447	370	4660	51.2
5	333	394	305	7410	0.1
4 and 5	339	445	376	4120	58.6

^a2.5 wt% doped films.

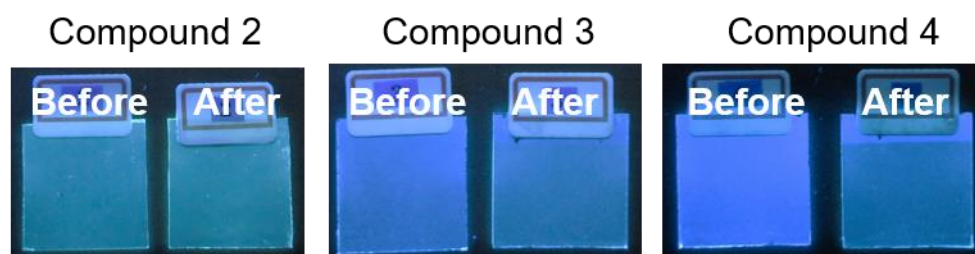


Fig. S6 The photographs under UV light (365nm) of PMMA films doped with **2-4** before and after simulated solar light irradiation.

6. NMR and MS spectra

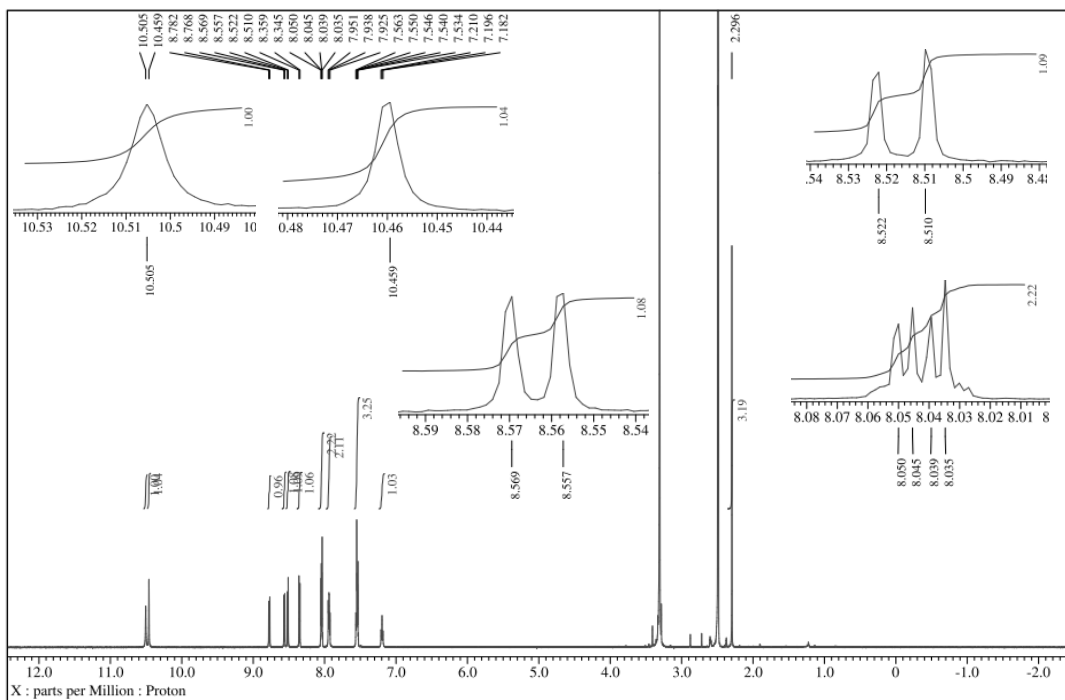


Fig. S7 ^1H NMR spectra of **1** (600 MHz, $\text{DMSO-}d_6$, 298K).

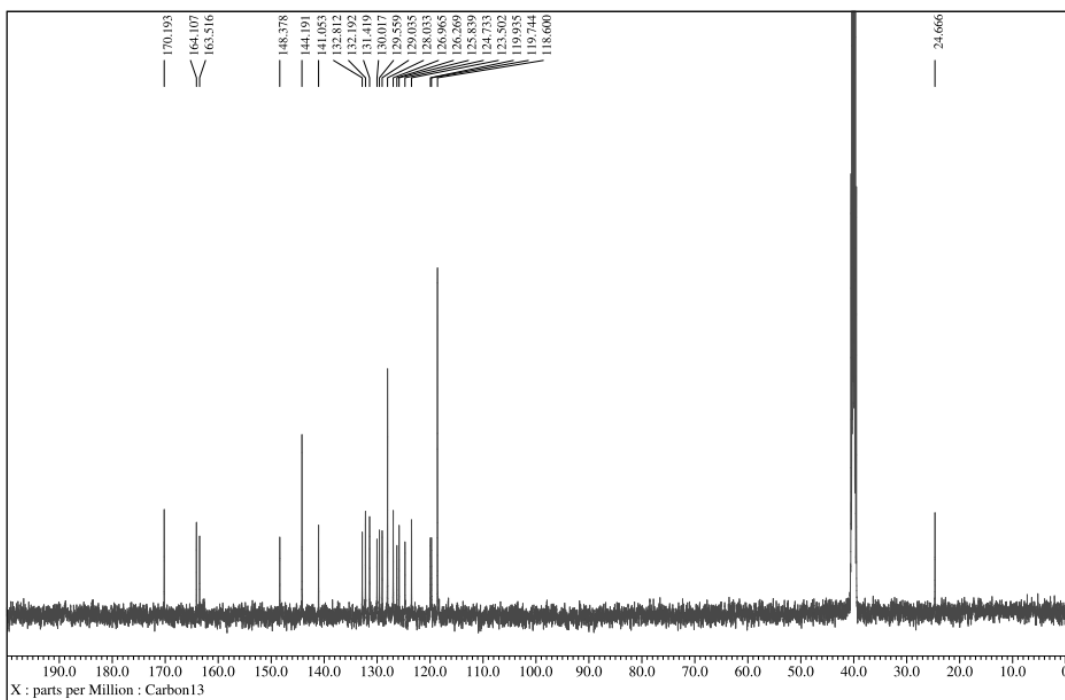


Fig. S8 ^{13}C NMR spectra of **1** (125 MHz, $\text{DMSO-}d_6$, 298K).

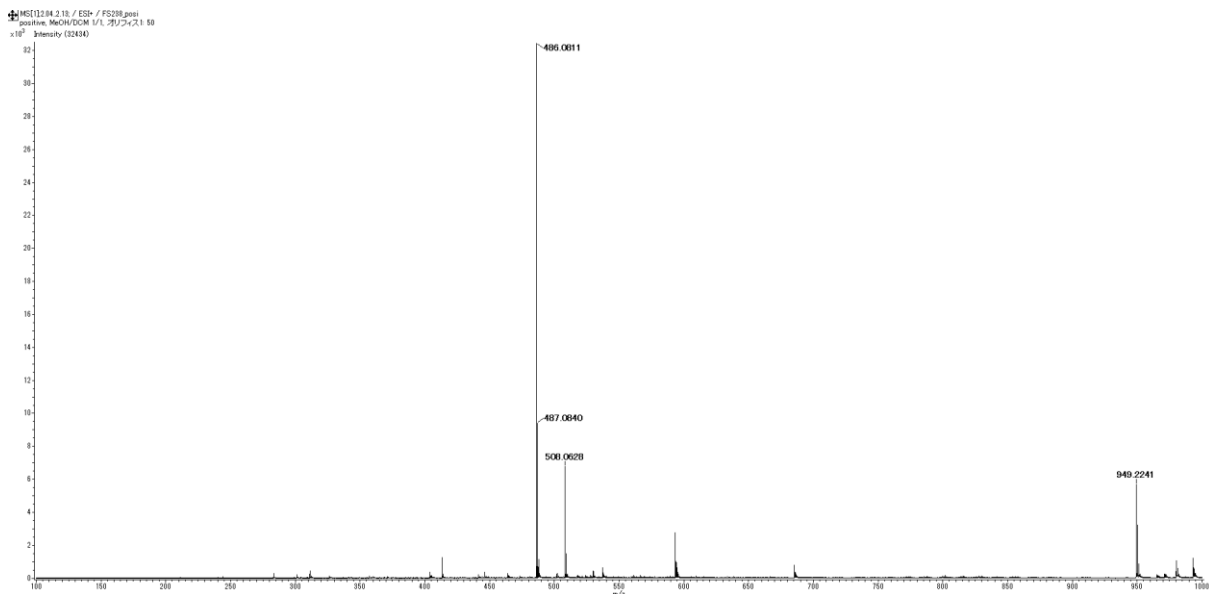


Fig. S9 ESI MS-spectra for **1**.

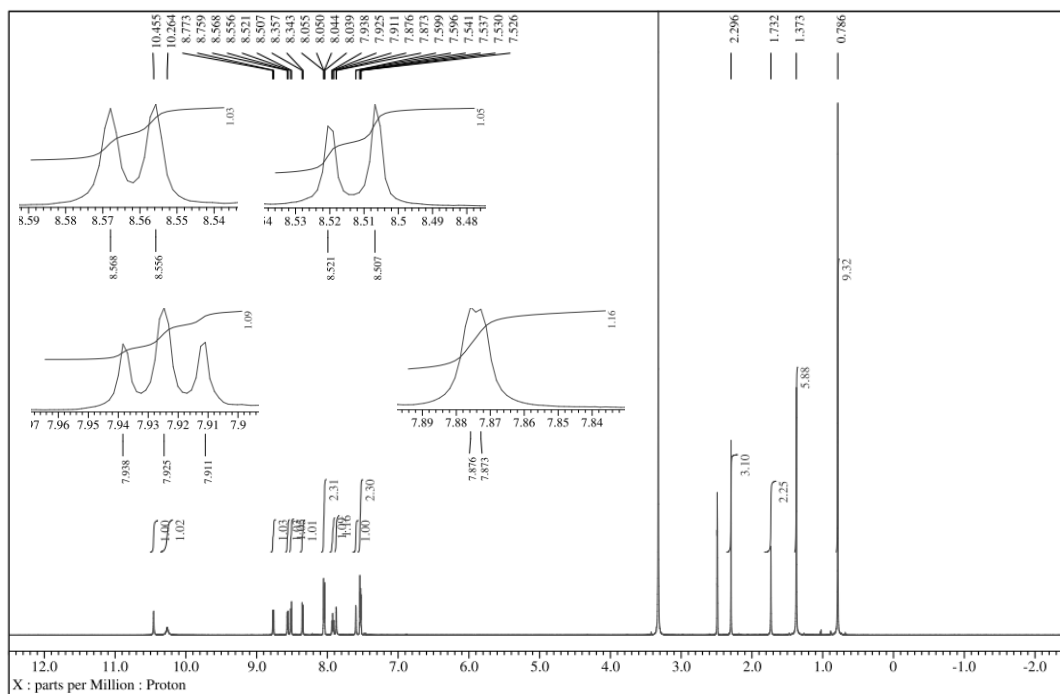


Fig. S10 ^1H NMR spectra of **2** (600 MHz, $\text{DMSO-}d_6$, 298K).

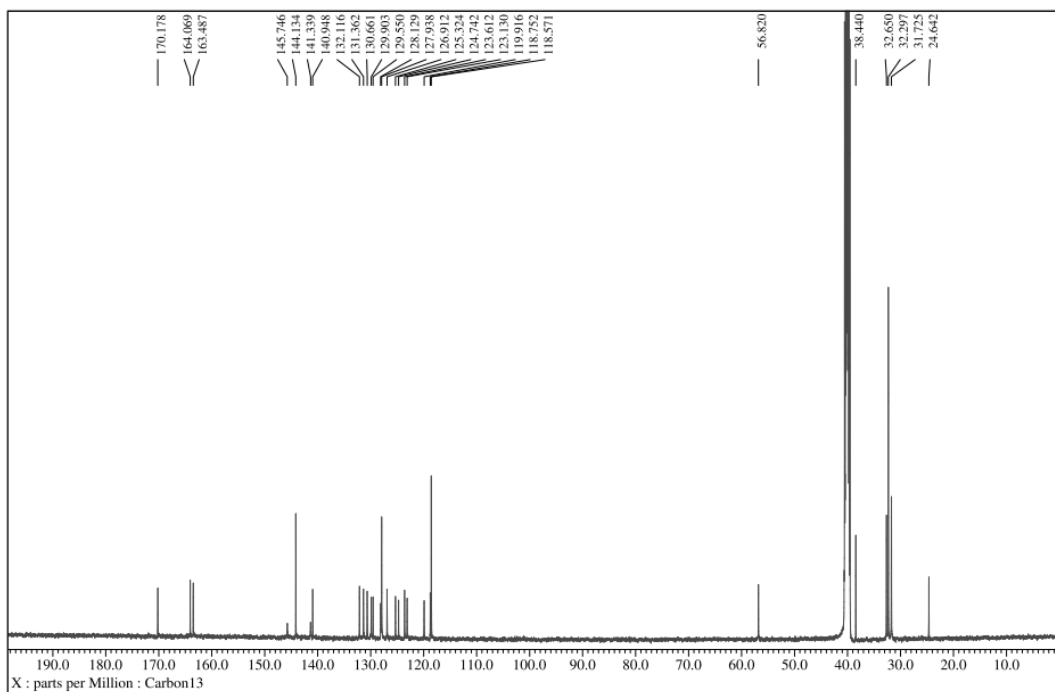


Fig. S11 ^{13}C NMR spectra of **2** (125 MHz, $\text{DMSO-}d_6$, 298K).

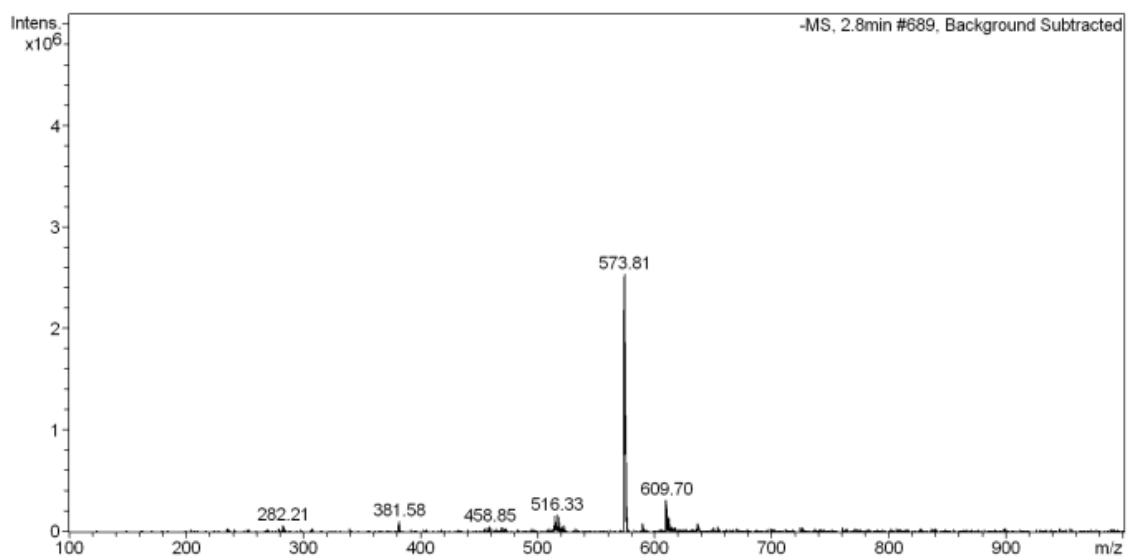


Fig. S12 ESI MS-spectra for **2**.

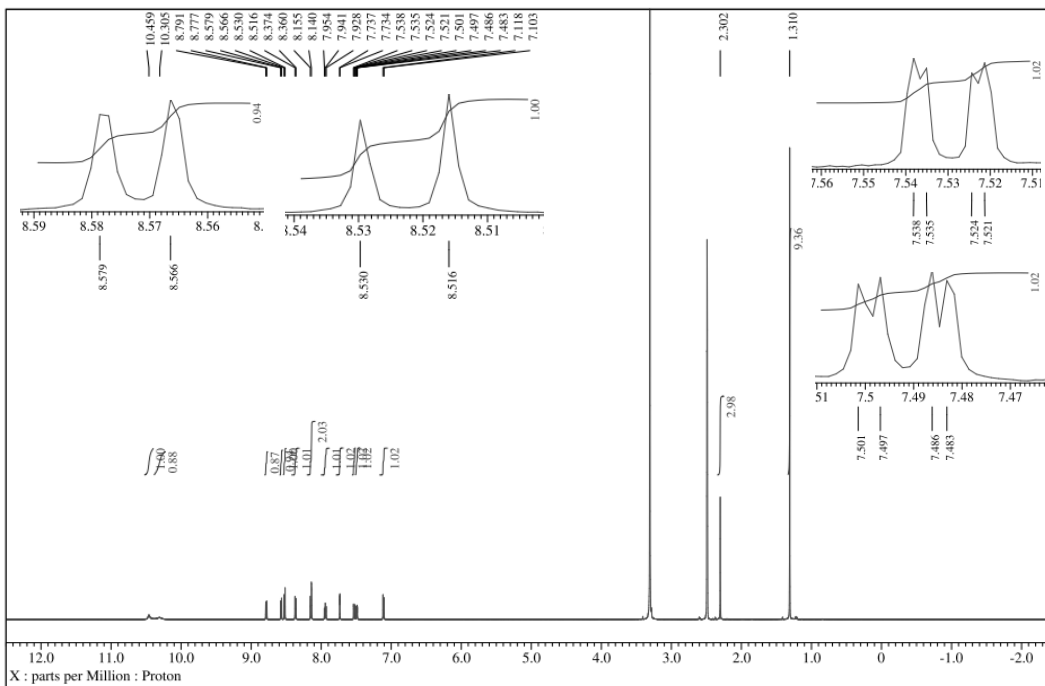


Fig. S13 ^1H NMR spectra of **3** (600 MHz, $\text{DMSO-}d_6$, 298K).

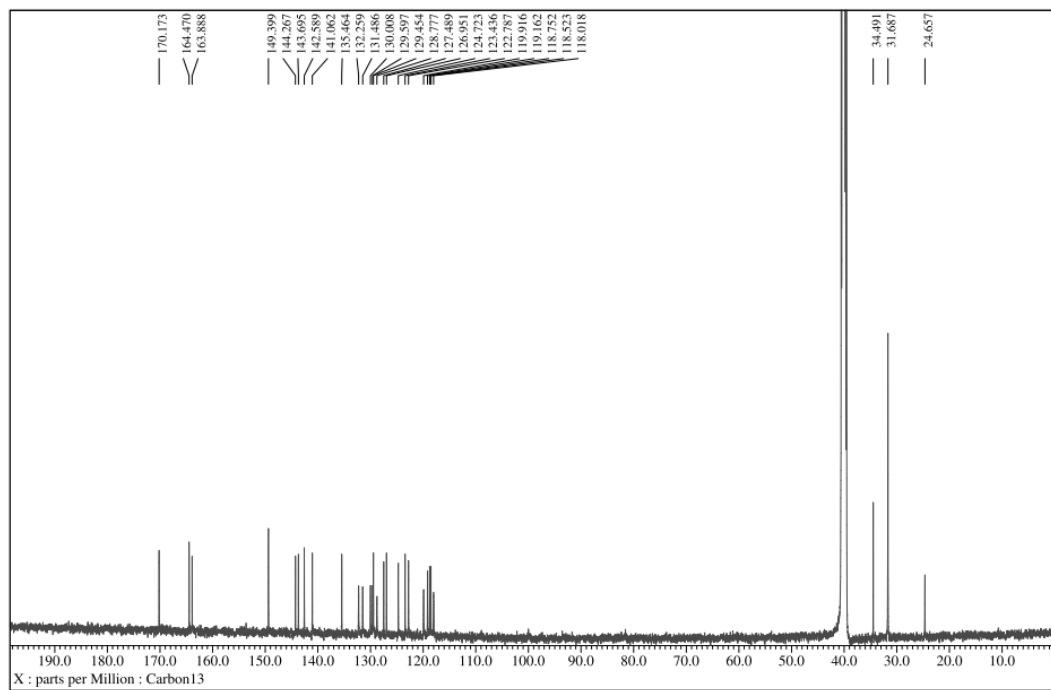


Fig. S14 ^{13}C NMR spectra of **3** (125 MHz, $\text{DMSO-}d_6$, 298K).

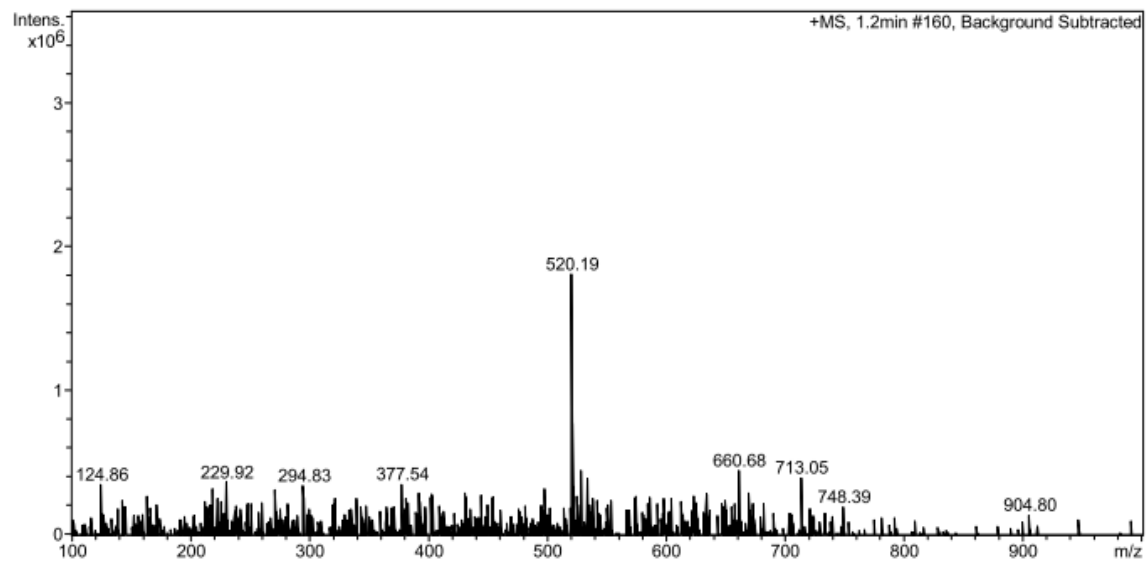


Fig. S15 ESI MS-spectra for **3**.

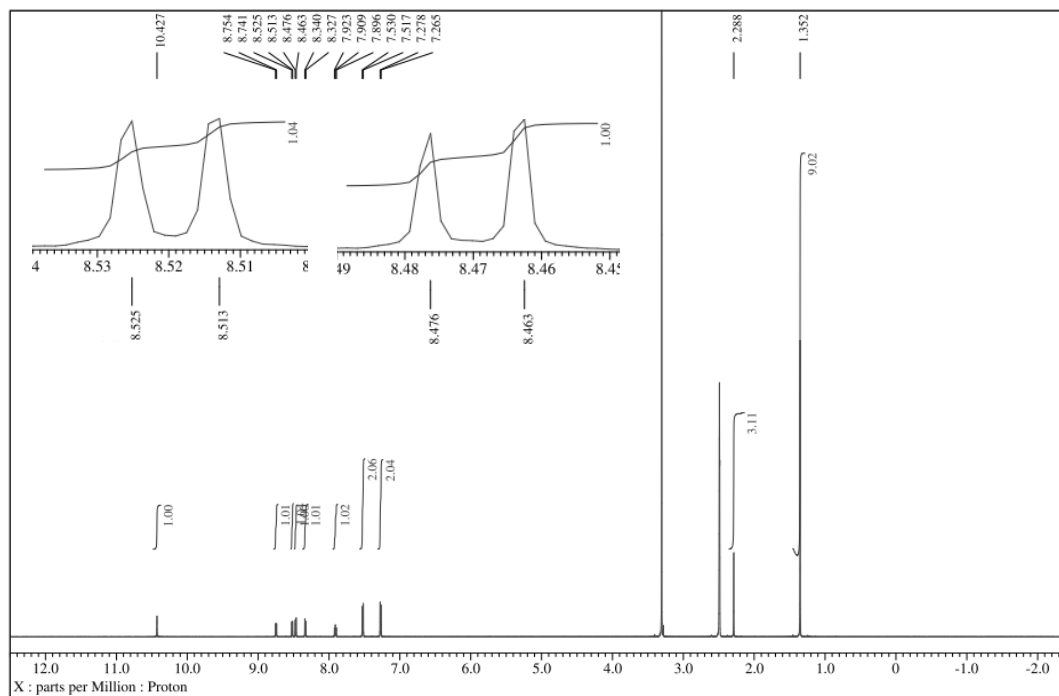


Fig. S16 ¹H NMR spectra of **4** (600 MHz, DMSO-*d*₆, 298K).

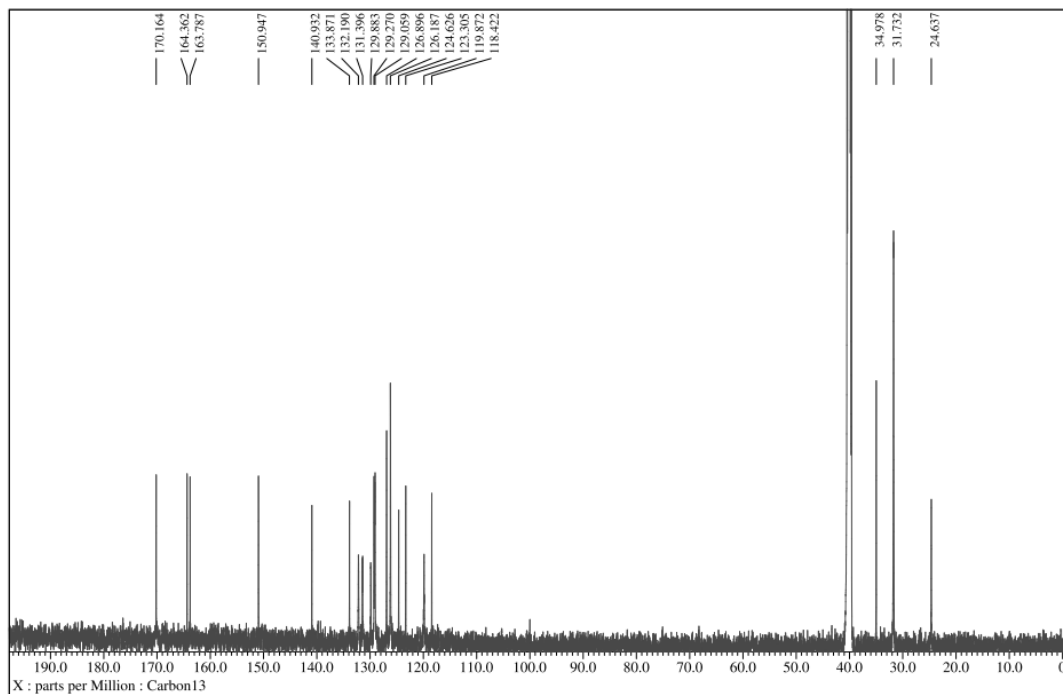


Fig. S17 ^{13}C NMR spectra of **4** (150 MHz, $\text{DMSO-}d_6$, 298K).

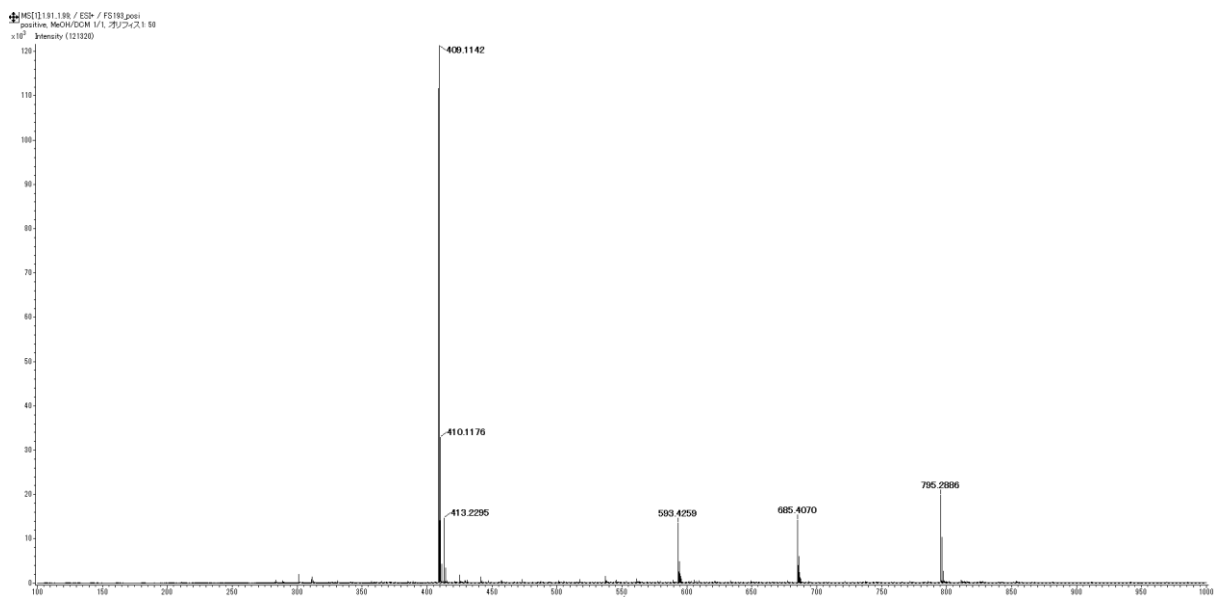


Fig. S18 ESI MS-spectra for **4**.

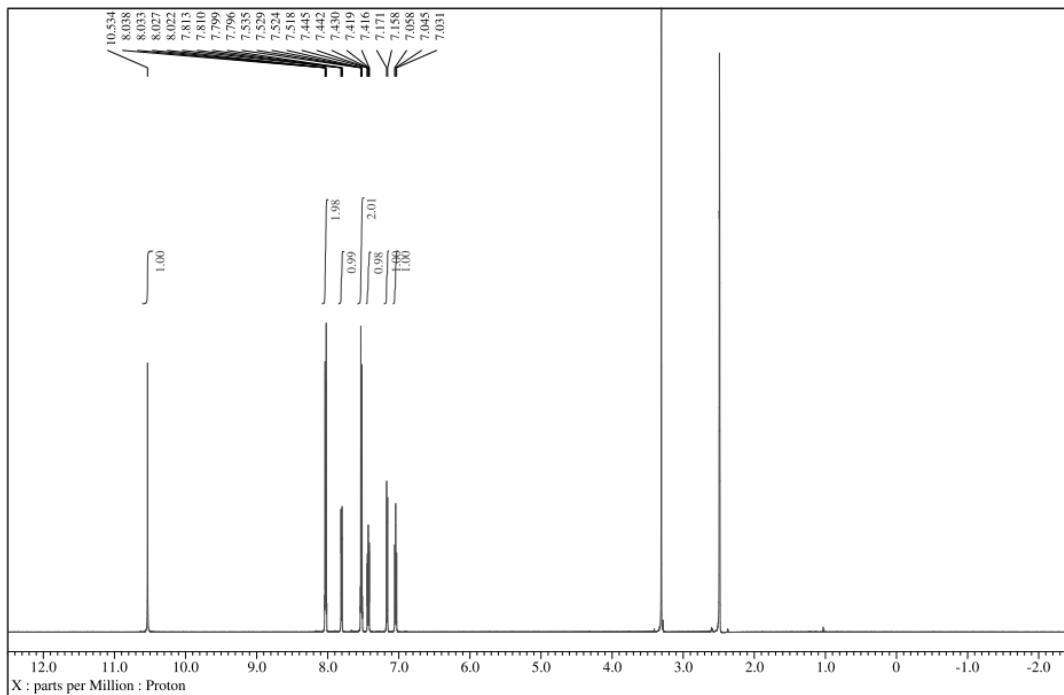


Fig. S19 ^1H NMR spectra of **5** (600 MHz, $\text{DMSO-}d_6$, 298K).

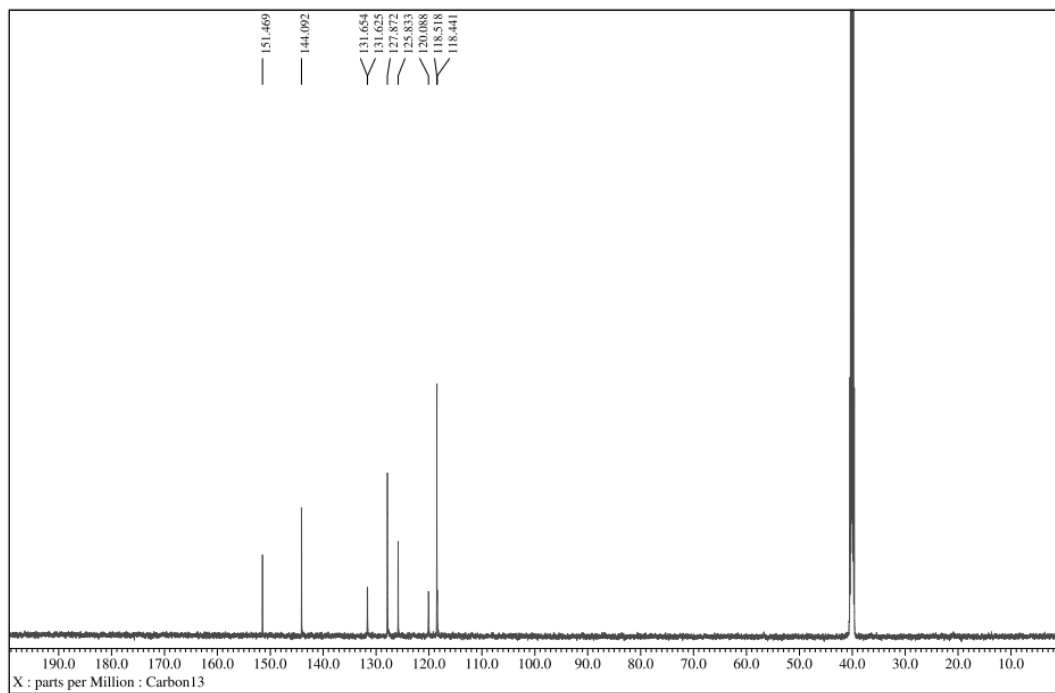


Fig. S20 ^{13}C NMR spectra of **5** (150 MHz, $\text{DMSO-}d_6$, 298K).

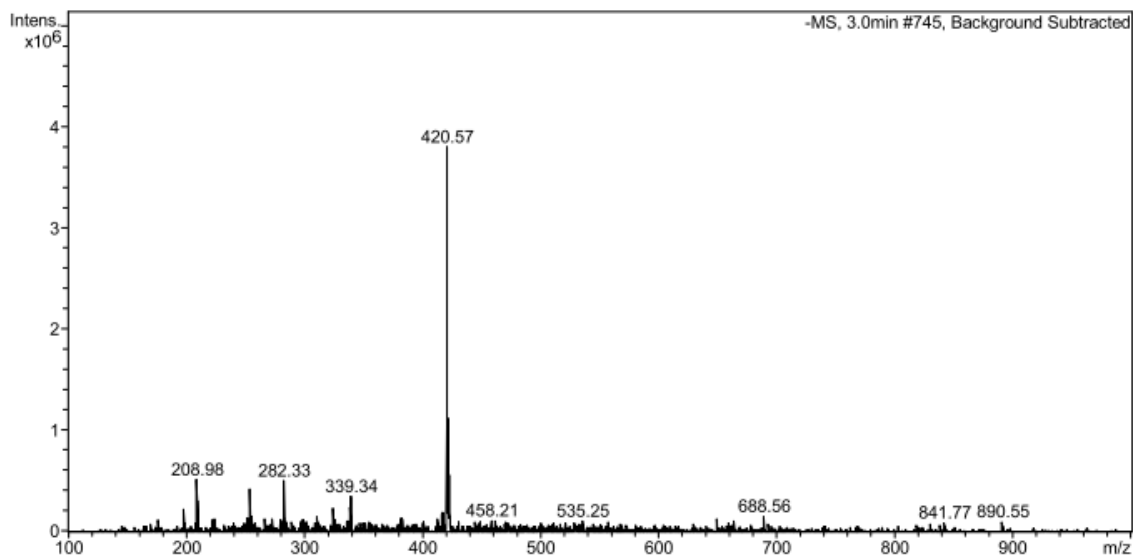


Fig. S21 ESI MS-spectra for **5**.

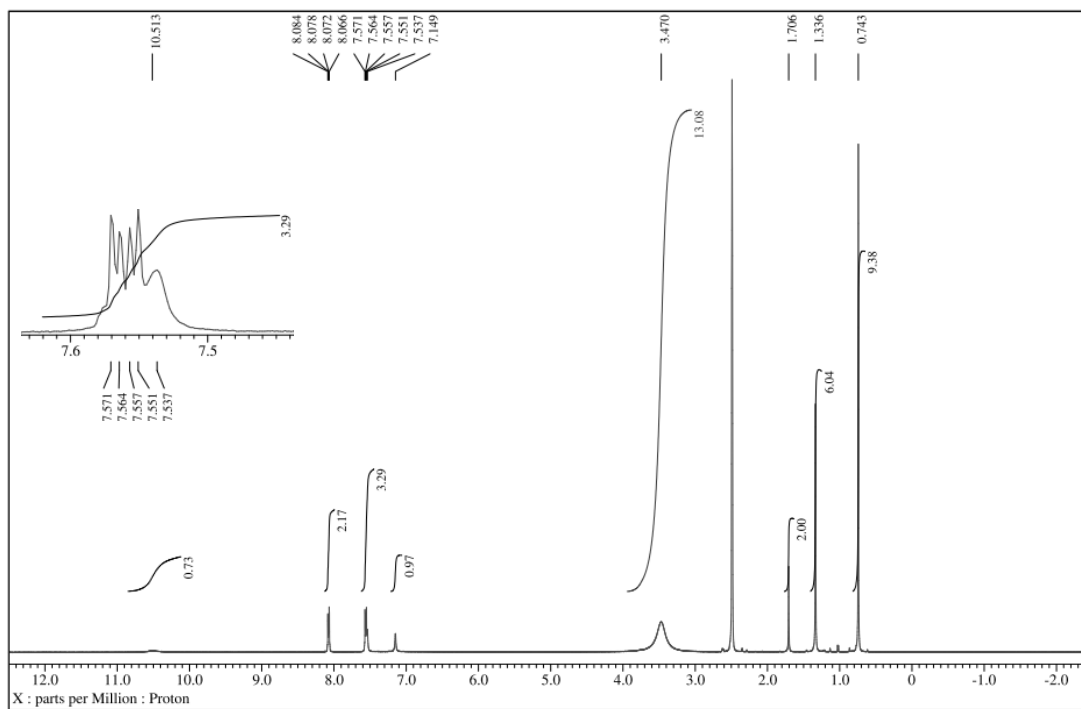


Fig. S22 ¹H NMR spectra of **6** (500 MHz, DMSO-*d*₆, 298K).

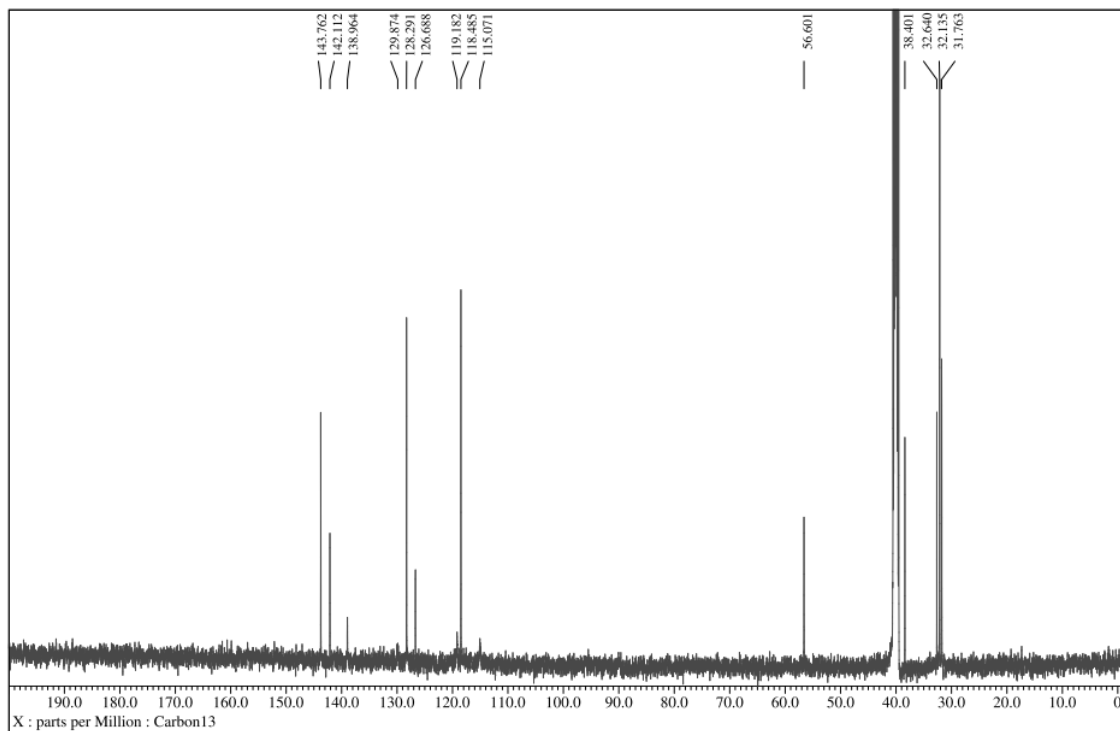


Fig. S23 ^{13}C NMR spectra of **6** (125 MHz, $\text{DMSO-}d_6$, 298K).

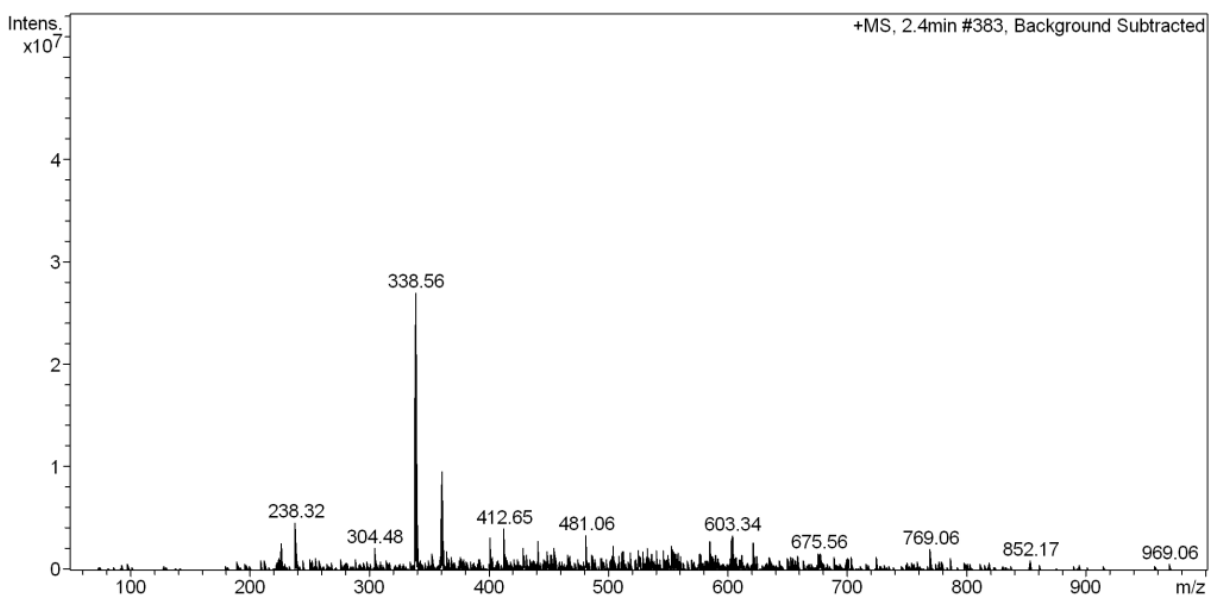


Fig. S24 ESI MS-spectra for **6**.

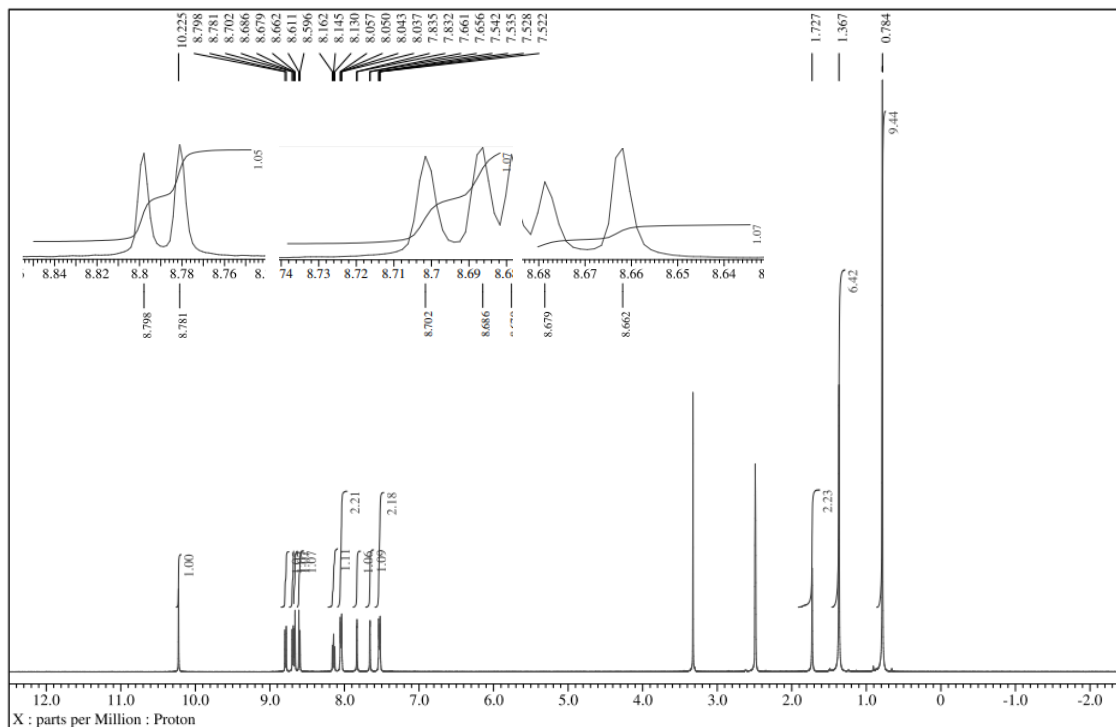


Fig. S25 ^1H NMR spectra of **7** (500 MHz, DMSO-d_6 , 298K).

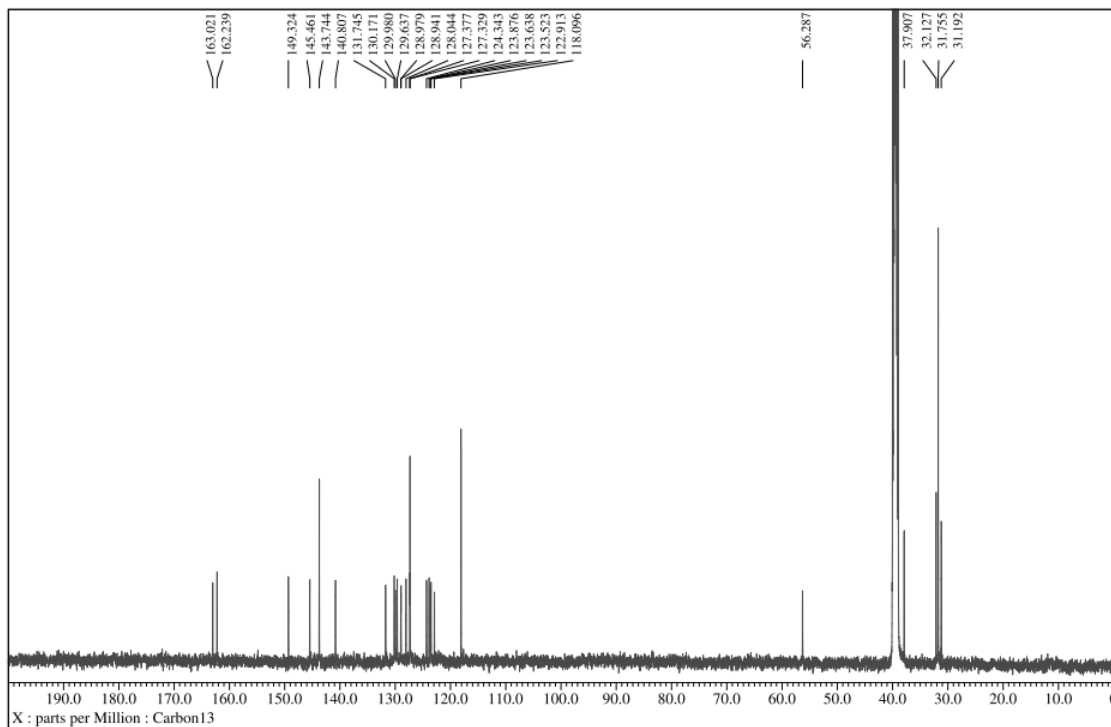


Fig. S26 ^{13}C NMR spectra of **7** (125 MHz, DMSO-d_6 , 298K).

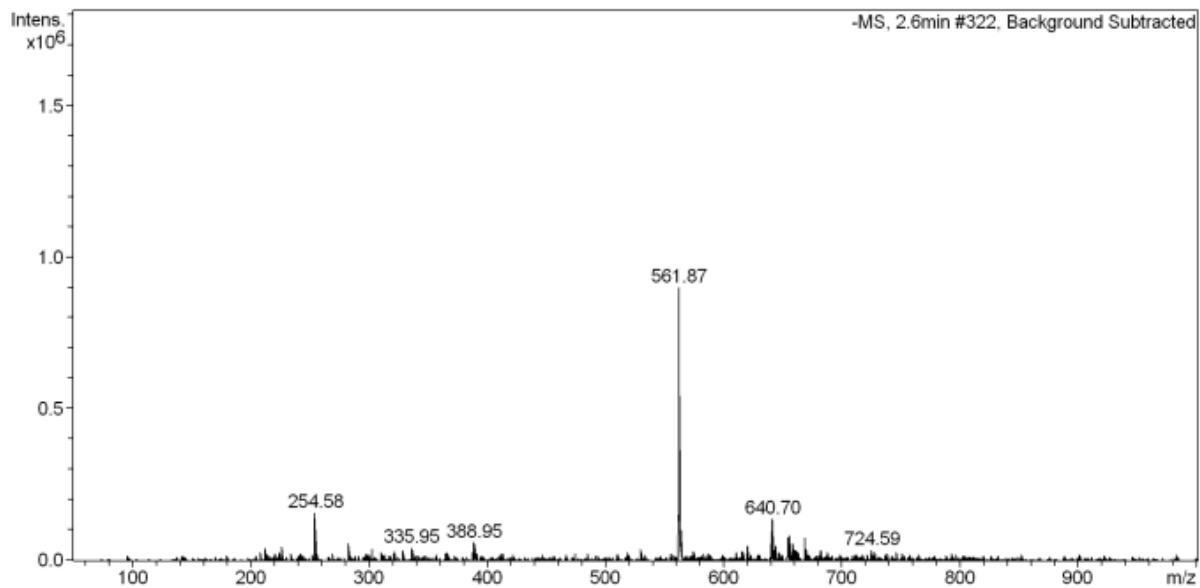


Fig. S27 ESI MS-spectra for **7**.

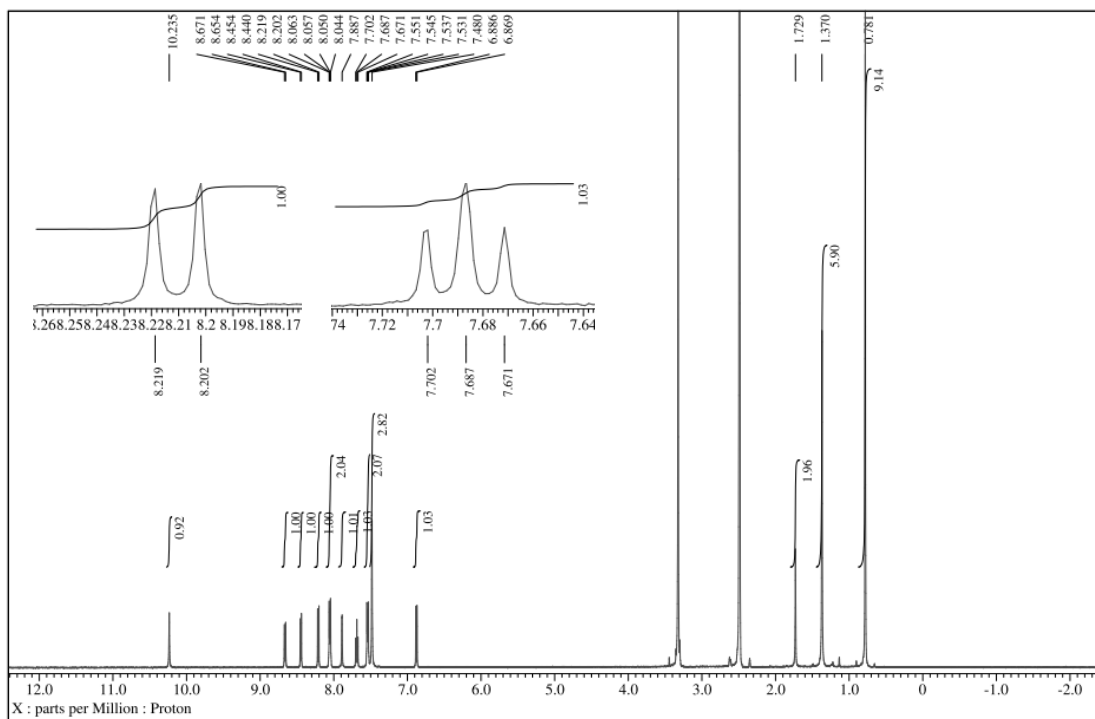


Fig. S28 ¹H NMR spectra of **8** (500 MHz, DMSO-*d*₆, 298K).

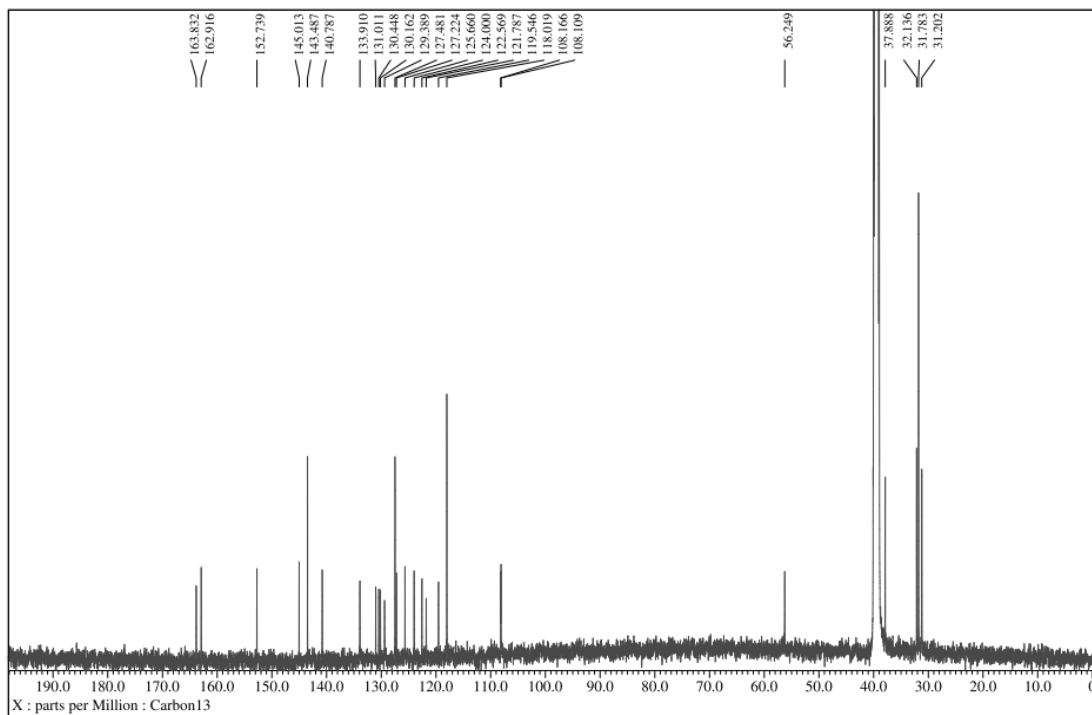


Fig. S29 ^{13}C NMR spectra of **8** (125 MHz, $\text{DMSO-}d_6$, 298K).

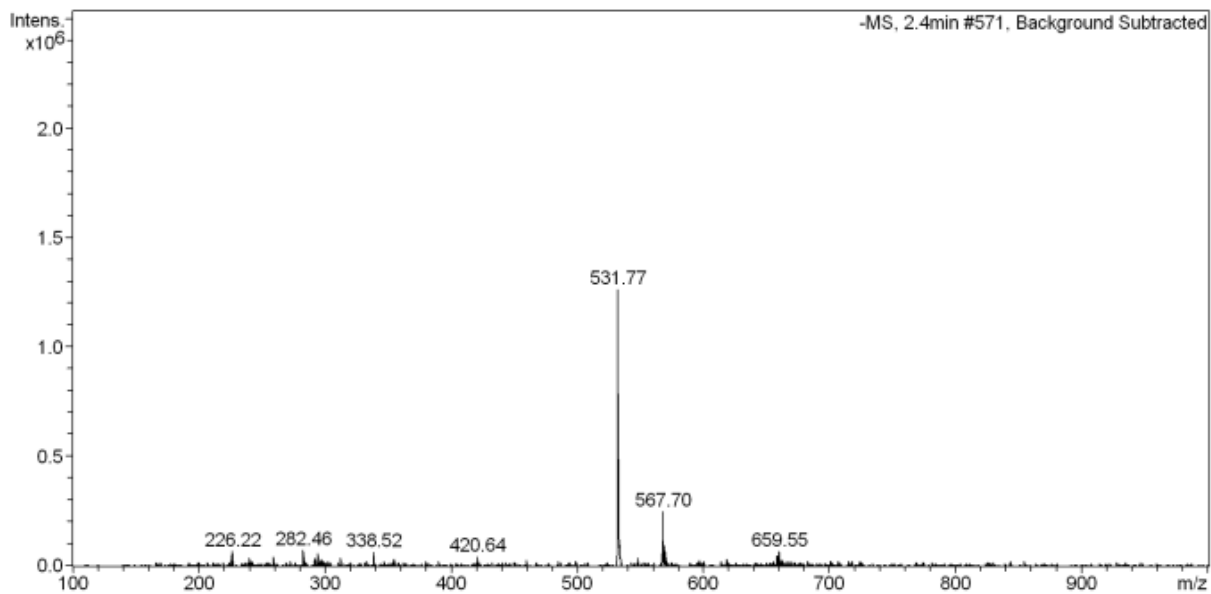


Fig. S30 ESI MS-spectra for **8**.

References

1. Gaussian 09, Revision **A.1**, Frisch, M. J.; Trucks, G. W.; Schlegel, H. B.; Scuseria, G. E.; Robb, M. A.; Cheeseman, J. R.; Scalmani, G.; Barone, V.; Mennucci, B.; Petersson, G. A.; Nakatsuji, H.; Caricato, M.; Li, X.; Hratchian, H. P.; Izmaylov, A. F.; Bloino, J.; Zheng, G.; Sonnenberg, J. L.; Hada, M.; Ehara, M.; Toyota, K.; Fukuda, R.; Hasegawa, J.; Ishida, M.; Nakajima, T.; Honda, Y.; Kitao, O.; Nakai, H.; Vreven, T.; Montgomery, Jr., J. A.; Peralta, J. E.; Ogliaro, F.; Bearpark, M.; Heyd, J. J.; Brothers, E.; Kudin, K. N.; Staroverov, V. N.; Kobayashi, R.; Normand, J.; Raghavachari, K.; Rendell, A.; Burant, J. C.; Iyengar, S. S.; Tomasi, J.; Cossi, M.; Rega, N.; Millam, N. J.; Klene, M.; Knox, J. E.; Cross, J. B.; Bakken, V.; Adamo, C.; Jaramillo, J.; Gomperts, R.; Stratmann, R. E.; Yazyev, O.; Austin, A. J.; Cammi, R.; Pomelli, C.; Ochterski, J. W.; Martin, R. L.; Morokuma, K.; Zakrzewski, V. G.; Voth, G. A.; Salvador, P.; Dannenberg, J. J.; Dapprich, S.; Daniels, A. D.; Farkas, Ö.; Foresman, J. B.; Ortiz, J. V.; Cioslowski, J.; Fox, D. J. Gaussian, Inc., Wallingford CT, 2009.